Co-gasification of woody biomass and chicken manure: syngas production, biochar reutilization, and cost-benefit analysis

Wei Cheng Ng[1], Siming You[1], Ran Ling[2], Karina Yew-Hoong Gin[2], Yanjun Dai[3], Chi-Hwa Wang[4*]

[1] NUS Environmental Research Institute, National University of Singapore,
1 Create Way, Create Tower #15-02, Singapore 138602
[2] Department of Civil and Environmental Engineering, National University of Singapore, 1 Engineering Drive 2, Singapore 117576
[3] School of Mechanical Engineering, Shanghai Jiaotong University,
Shanghai, China 200240
[4] Department of Chemical and Biomolecular Engineering, National University of Singapore, 4 Engineering Drive 4, Singapore 117585

*Corresponding author: Tel.: +65-65165079; Fax: +65-67791936; E-mail address: chewch@nus.edu.sg (C. H. Wang).

Submitted for publication to

Energy

March 2017

Abstract

The management and disposal of livestock manure has become one of the top environmental issues at a global scale in line with the tremendous growth of poultry industry over the past decades. In this work, a potential alternative method for the disposal of chicken manure from Singapore local hen layer farms was studied. Gasification was proposed as the green technology to convert chicken manure into clean energy. Through gasification experiments in a 10 kW fixed bed downdraft gasifier, it was found that chicken manure was indeed a compatible feedstock for gasification in the presence of wood waste. The co-gasification of 30 wt% chicken manure and 70 wt% wood waste produced syngas of comparable quality to that of gasification of pure wood waste, with a syngas lower heating value (LHV) of 5.23 MJ/Nm^3 and 4.68 MJ/Nm^3, respectively. Furthermore, the capability of the gasification derived biochar in the removal of an emerging contaminant (artificial sweetener such as Acesulfame, Saccharin and Cyclamate) via adsorption was also conducted in the second part of this study. The results showed that the biochar was effective in the removal of the contaminant and the mechanism of adsorption of artificial sweetener by biochar was postulated to be likely via electrostatic interaction as well as specific interaction. Finally, we conducted a cost-benefit analysis for the deployment of a gasification system in a hen layer farm using a Monte Carlo simulation model.

Keywords: gasification; chicken manure; biochar, adsorption; emerging contaminants; cost-benefit analysis.

1. Introduction

Due to the tremendous growth of poultry industry over the past decades, the management and disposal of livestock manure has become one of the top environmental issues at a global scale [1]. An estimate by the United States Department of Agriculture (USDA) showed that farms in the United States produce more than 335 million tonnes of dry matter waste annually [2]. This huge amount of animal manure if not properly disposed of, may lead to air pollution due to the release of gases such as hydrogen sulphide and ammonia [3]. The leaching of manure by rainwater followed by runoff of the leachate, or the presence of pathogens in the manure, could also potentially result in the contamination of soil and water resources, which eventually will affect human health [1].

In Singapore, there are three hen layer farms which cater for about one fourth of the total egg demand, i.e., around 1.2 million/day [4]. These farms inevitably generate over 200 tonnes of animal waste on a daily basis, the disposal of which poses a potential challenge. Specifically, Chew's Agriculture rears approximately 750,000 chickens that generate 60 tonnes of chicken manure per day, while Seng Choon Farm produces about 70 to 80 tonnes of chicken manure per day [5]. One of the potential ways to dispose of the animal manure is incineration [6]. However, the incineration of manure produces a cocktail of toxic by-products (e.g., dioxins and furans) that are harmful to the environment and general public health if not appropriately controlled [7]. There is a need to develop or apply alternative technologies to treat or contain this dairy biomass.

Gasification is gaining increasing attention in the waste-to-energy or renewable energy research field as it is regarded as a green technology that could potentially be an alternative solution to incineration in the disposal of the chicken manure. It has been showcased in a number of studies that gasification is capable of treating a diverse source of solid waste such as sludge, wood and horticultural waste, food waste, dairy manure, and etc. [8-11] with encouraging results. Since gasification is conducted in an oxygen deficient environment as opposed to the oxygen-rich environment in incineration, the formation of the toxic pollutants is effectively restrained [9, 12]. Furthermore, the gasification technique is well suitable for a decentralised application [13]. On-site treatment of chicken manure at the farms will benefit in two ways: (1) the environmental concerns (e.g., pathogen transmission and odour spread) during the transport of chicken manure to incineration plants is avoided; (2) the power generation (e.g., electricity converted from syngas) from gasification could be used to satisfy a part of the energy demand of the farms. Furthermore, while syngas could also be used for synthesis of valuable hydrocarbons via the Fischer-Tropsch process, a water-gas shift reaction ($CO + H_2O \rightleftharpoons CO_2 + H_2$) is required to adjust the syngas to an ideal H_2:CO ratio of 2:1 beforehand, typically done in the industry first through a high temperature shift followed by a low temperature shift to maximize CO conversion [14]. Last but not least, gasification also produces valuable solid products such as biochar and ash at the end of the process [15, 16] which have a great application potential in multiple fields including building and construction, agriculture, water treatment, catalysis and etc. [17-19]. For example, biochar can be mixed into soil for agricultural purposes to enhance soil quality and nutrient content [20, 21]. Because of its low bulk density [22], biochar could also be mixed into concrete as construction material and offers the benefits of light weight and carbon sequestration capability [23].

Recently, the capability of biochar in the adsorption and removal of some pollutants such as heavy metals and organic contaminants in water streams is also well-recognized [18, 24]. As a newly recognized class of emerging contaminants, the artificial sweetener (AS) such as

Acesulfame, Saccharin, Cyclamate, and etc., in water streams pose a potential threat to ecosystems because it is extremely persistent and resistant to conventional waste water treatment processes [25, 26]. Its continuous introduction into the water environments has caused an accumulation in many aquatic ecosystems. Previous studies have shown that AS may change the physiology and locomotion of *Daphnia magna* [27], and interfere with plant photosynthesis [28]. However, since conventional approach is not very effective in the removal of AS from water streams [29, 30], there is a need to explore alternative methods that are cost effective yet environmentally friendly. One possible solution is to use biochar that is derived from solid waste through the gasification technology. The successful adsorption of AS by the biochar derived from the gasification of chicken manure will add a further economic benefit from biochar sale to the farms.

In this work, the feasibility of applying the gasification technology for the on-site disposal of chicken manure at hen layer farms is explored. The performance of the co-gasification between chicken manure and wood chips is assessed, with the quality of syngas produced being the indicator. The capability and mechanism of gasification-derived biochar in adsorbing and removing AS from water are studied. Lastly, a cost-benefit analysis is conducted to showcase the economic viability of the on-site application of gasification systems at the farms. Overall, this work aims to show that gasification system as a whole is a robust technology for waste reduction, energy harvesting, valuable solid product generation.

2. Materials and Methods

2.1 Feedstock preparation

Chicken manure collected from a local chicken farm was first dried at 68^{o}C for 24 hours in a dehydrator (Excalibur Parallex 9 Trays commercial dehydrator) to remove its free moisture content. The chicken manure moisture content after drying was approximately 10 wt%. The dried manure was then used for subsequent characterization and gasification experiment. The mesquite wood chips (Kingsford Manufacturing Co., USA) used for mixing with chicken manure prior to co-gasification were approximately 2.54-3.81 cm in size. Two types of final feedstock were prepared for gasification/ co-gasification: (i) 100 wt% wood chips (100%WC), and (ii) 30 wt% chicken manure + 70 wt% wood chips mixture (30%CM+70%WC). The reason for using a 30 wt% chicken manure in the mixture was to avoid bridging in the hopper based on our past experience that feedstock with sizes below the lower limit (1.27 cm) has a higher likelihood of blocking the hopper, hence obstructing the flow of feedstock down the reactor [11].

2.2 Feedstock characterization

Proximate analysis and ultimate analysis were performed on chicken manure and wood chips. For proximate analysis of feedstock, a Thermal Gravimetric Analyzer (TGA) (Shimadzu, DTG-60A) was employed where the feedstock sample was heated from 25^{o}C to 800^{o}C at a rate of 20^{o}C/minute in nitrogen or air atmospheres. The TGA profile was then used to identify the moisture, volatiles, fixed carbon and ash contents of feedstock.

For ultimate analysis, a Vario MACRO Cube elemental analyzer was used to determine the carbon, hydrogen, nitrogen and sulphur content of the feedstock. Briefly, approximately 2-3g of sample was combusted at 1150^{o}C to produce CO_2, H_2O, NO_2, and SO_2 gases, and the gas detector would detect and analyze the mass percentage of each element (C, H, N and S). The mass percentage of oxygen was estimated by subtracting C, H, N, S and ash content mass percentages from 100%. The higher heating value (HHV) of each feedstock was subsequently estimated using Eq. (1) [31]:

$$HHV = 0.3491*M_C + 1.1783*M_H + 0.1005*M_S - 0.1034*M_O - 0.0151*M_N - 0.0211*M_{ash} \quad (1)$$

where M_i is the mass percentage of the element i (i.e. i = C, H, N, S, O and ash).

2.3 Co-gasification experiment

The gasifier used in this experiment was a 10kW fixed-bed downdraft gasifier with a feedstock intake rate of 10kg/h (All Power Labs, Berkeley, CA). Figure 1(a) shows the schematic of the gasifier. The feedstock was first introduced into the hopper located at the top of the gasifier and the vacuum fan was switched on. Then the gasifier was started up by introducing and igniting some gasoline at the igniter to heat up the reactor. Upon reaching a temperature range of ~800-900°C, the rotating auger was initiated to feed the feedstock into the gasifier at a rate of 10kg/h, where the feedstock went through four zones of reactions namely drying, pyrolysis, combustion and reduction (gasification). Air flow into the combustion zone of the reactor was regulated through a nozzle to control the temperature where necessary. The air flow rate in the experiment was 4L/s. Upon reaching a steady state operation (approximately 850°C in the reduction zone and 900°C in the combustion zone with no significant fluctuation), the syngas produced was tapped from the gas sampling port and filtered before it was analysed by a Gasboard 3100P gas analyser to measure the CO, H_2, CO_2, CH_4, O_2 content and the lower heating value (LHV) of the syngas. For every batch of the experiment, the residence time of the feedstock in the gasifier was roughly 3 hours. While the downstream syngas to power generation section was not covered in the scope of this work, a more complete schematic was proposed (process flowsheet in Figure 1(a)) and details were further outlined in Section 2.6 to allow a more thorough analysis of the deployment of gasification system in hen layer farms.

2.4 Characterization of biochar

The morphological structure of the biochar produced from gasification was observed with a scanning electron microscope (SEM) (JEOL JSM 5600LV). The surface area and porosity of biochar was analysed with a Brunauer–Emmett–Teller (BET) test. Proximate and ultimate analyses were also performed on biochar based on the procedures described in Section 2.2. The pH of the biochar was determined with a SI Analytics Lab 870 pH meter by suspending 1g of biochar in 10ml of deionized water.

2.5 Adsorption of artificial sweetener (AS)

2.5.1 Kinetics and isotherms study of adsorption of AS by biochar

The three species of artificial sweeteners (AS) of interest, acesulfame (ACE), saccharin (SAC) and cyclamate (CYC), were purchased from Sigma-Aldrich Pte. Ltd., Singapore. These three AS species were chosen as they are very commonly studied in research owing to their presence in many water systems [26, 32]. For kinetics study, 10mg of biochar was suspended in 5ml of 100ppb AS (dissolved in deionized water) in 15ml centrifuge tubes. The tubes were left shaking at 150rpm and 25^{o}C for different durations. At pre-determined time points (every 30 minutes, up to 6 hours), the tubes were retrieved from the shaker and the contents filtered to separate the solid biochar and liquid AS. 100ppb AS solutions in 15ml centrifuge tubes without the addition of biochar were used as the respective controls for each time point. The filtrate was then sent for LC-MS/MS analysis to determine the concentration of AS using a similar method in our previous work [33].

For isotherms study, 10mg of biochar was suspended in 5ml of AS of different initial concentrations (10-100ppb) for 6 hours. After 6 hours of shaking, the filtrate was analysed with LC-MS/MS using the method described above to determine the concentration of AS, which was also the equilibrium concentration. AS solution in the absence of biochar was used as a control. All experiments were conducted in triplicates.

2.5.2 Effect of pH and water hardness on adsorption capacity

To investigate the effect of pH on the adsorption capacity in an attempt to investigate the mechanism of adsorption, 10mg of biochar was suspended in 5ml of 100ppb AS in 15ml tubes. Then the suspension pH was adjusted by the dropwise addition of HCl or NaOH to a pH range of 3-10 (SI Analytics Lab 870 pH meter). As the dropwise addition was done with a 10μl pipette and 6-8 drops were added to each sample on average, the influence to the overall concentration was assumed to be negligible. The suspensions were shaken at 150rpm and 25^{o}C for 6 hours. After that, the suspension pH was re-measured (due to the buffering capacity of the biochar) and the suspension was filtered. The AS concentration of the filtrate was measured by LC-MS/MS. Meanwhile, to study the effect of water hardness, 10mg of biochar was suspended in 5ml of 100ppb AS in water of different total hardness (as $CaCO_3$ mg/L): DI water (0 mg/L), Singapore tap water (66 mg/L on average [34]), mixture of DI and tap water in 1:1 ratio (~33 mg/L), seawater (~6630 mg/L [35]), and 10× diluted seawater (~663 mg/L). Similar to the above, the suspension was filtered after adsorption and the AS concentration of the filtrate was measured by LC-MS/MS.

2.5.3 Effect of pH on zeta potential of AS-biochar suspension

To determine whether specific bonding between AS molecules and biochar surface (that can result in a change in the overall biochar surface charge) is a possible mechanism of adsorption, the zeta potential of AS-biochar suspension was measured. The zeta potential of biochar in deionized water or 100ppb AS at different pH was determined by suspending 10 mg of biochar in 40 mL of deionized water or AS. The suspension pH was adjusted to within the range of 3 – 8 with HCl or NaOH (SI Analytics Lab 870 pH meter). Similarly, the total volume of acid or base added was negligible as compared to the final suspension volume. Following pH adjustment, the suspension was sonicated for 30 minutes at 25^{o}C in an ultrasonic bath unit (Elma S30H), and subsequently allowed to stand for 2 days before the zeta potential was measured with Malvern Zetasizer Nano ZS. The suspension pH was also re-measured when measuring the zeta potential.

2.6 Cost-benefit analysis

2.6.1 Scheme Proposal and Parameter Selection

A complete schematic of the whole gasification plant to be set up in the farm is proposed (presented in Figure 1(a)) to facilitate a more thorough analysis of the technology from the starting point (feedstock) to electricity generation. After the gasification of feedstock to produce syngas as discussed in section 2.3, the syngas is cleaned up via a series of processing units such as cyclone, cooler and scrubber to remove fine particulates and impurities. Thereafter, cleaned syngas is fed to a gas engine to generate electricity. The power output is calculated as [36]

$$P = \dot{m}_{biomass} \times LHV_{\text{feedstock}} \times CGE \times EF \quad (2)$$

where $\dot{m}_{biomass}$ is the biomass consumption rate (kg/h); $LHV_{\text{feedstock}}$ (MJ/kg) is the lower heating value of feedstock; CGE is the cold gas efficiency; EF is the electrical efficiency of the gas engine. $LHV_{\text{feedstock}}$ and CGE are obtained based on our experiments.

Based on the design of the plant proposed above, a cost-benefit analysis for the deployment of a gasification system in one of the hen layer farms is conducted following a similar scheme employed by the study of You et al. [13]. The cost components involved in the gasification-based disposal include the initial capital investment such as the facility and land costs, operating and maintenance (O&M) cost, woodchip cost, cost contingency, and external costs. However, for the case of hen layer farms, the existing, spacious land space makes the land cost negligible, that is, no extra land space needs to be purchased for the gasification system. We consider to use commercial woodchips as co-gasification agents instead of existing horticultural or wood waste as proposed in the study by You et al. [13]. The woodchips do not need to go through a pre-treatment process and could be directly used for gasification as we did during the experiments. The bulky and loose form of horticultural or wood waste and the large demand of co-gasification agent further makes the use of horticultural or wood waste less realistic for a hen layer farm. The cost contingency is used to consider the costs that are unknown at the moment but will probably occur in the future. The external costs defined as the monetary valuation of damages caused by the pollutants emitted during a process are also negligible as suggested by previous studies [13]. Hence, the major cost components are the facility cost, O&M cost, woodchip cost, cost contingency. Note that the cost of the gasification system used in the CBA is an overall cost of the system based on the reference of the data, that is, it includes the cost of gasifier, syngas cleaning units, and electricity generation system. The O&M cost includes salaries, training cost, and component replacement cost, etc. The major benefit components include selling electricity (energy income), waste (chicken manure) disposal income, and biochar (resource income). To account for the underlying uncertainty of variable parameters, triangular distributions are assumed and the cost-benefit analysis is modeled by Monte Carlo simulation with a total of 10^5 iterations. The triangular distributions of the variable parameters are summarized in Table 1.

Similar to the study by You et al. [13], a triangular distribution with a lower limit, mode, and upper limit of 1000, 1500 and 2000 US$/kW, respectively, is set to be the unit cost of a gasification system (including both gasifier and gas engine sub-systems) in 2007. The cost is updated to the current year (2017) using the Chemical Engineering Plant Cost Index (CEPCI) as Eq. (3)

$$\mathrm{Cost}_i = \mathrm{Cost}_j(\mathrm{CEPCI}_i/\mathrm{CEPCI}_j) \tag{3}$$

where i and j denote the current year (2017) and base year (2007), respectively. The annual value of CEPCI for 2007 was 525.4, while the annual value of CEPCI for year 2017 is not available and is represented by that for 2015, i.e., 556.8. The scale dependence of facility cost is considered by Eq. (4) [37]

$$\mathrm{Cost}_k = \mathrm{Cost}_i(\mathrm{S}_k/\mathrm{S}_i)^f \tag{4}$$

where S_k and S_i denote the designed facility capacity and base facility capacity, respectively. Considering an operating time of 24 hours per day [38], the yearly mass of chicken manure of around 27000 tons [5], and a feedstock mixture ratio of 30% vs 70% between the chicken manure and woodchips, the full load capacity of the designed system is estimated to be around 3.1 MW with a feedstock consumption rate of 3.7 ton/hr. The base facility capacity was set to be 1 MW [39]. $f = 0.7$ is the scaling factor.

Similar to the study by You et al. [13], a triangular distribution with a lower limit, mode, and upper limit of 0.008, 0.014, and 0.02, respectively, is set for the ratio between the monthly O&M cost and the capital cost (i.e., the facility cost). It is assumed that the O&M cost increases at a rate of 5% [40]. The price of wood chips is set to be triangularly distributed with a lower limit, mode, and upper limit of 100, 150, and 200 US$/ton [41], respectively. The cost contingency is considered to have a triangular distribution with a lower limit, mode, and upper limit of 2, 4, and 6 US$/kW/year [40], respectively. The electrical efficiency of gas engine is considered to have a triangular distribution with a lower limit, mode, and upper limit of 25%, 30%, and 35%, respectively [42]. The syngas to power conversion efficiency is typically about 25% [43]. Electricity is also consumed by the gasification system itself, which is the so-called auxiliary electricity consumption (AEC). AEC is considered to be 10% [40]. A triangular distribution with a lower limit, mode, and upper limit of 0.1, 0.2, and 0.3 US$/kWh, respectively, is assumed for the tariff of electricity [44]. The waste income is estimated by the product of net waste handled by the gasification system and the refuse disposal fee. A triangular distribution with a lower limit, mode, and upper limit of 50, 60, and 70 US$/ton, respectively, is assumed for the refuse disposal fee [45]. Note the waste disposal benefit here denotes the cost that the farm otherwise needs to undertake if the chicken manure is disposed outside of the farm (i.e., by incineration). The price of biochar is set to be triangularly distributed with a lower limit, mode, and upper limit of 1000, 2500, and 4000 US$/ton, respectively, considering the global average biochar price is around 2650 US$/ton [46]. The mass of biochar is based on our experimental data as reported below.

The net present value (NPV) is calculated as Eq. (5)

$$\mathrm{NPV} = \sum_{t}^{LT} \frac{C_{it}}{(1+r)^t} - C_0 \tag{5}$$

where C_t is the net cash inflow during a year t; C_0 is the total initial capital investment; LT=20 denotes the life time of the gasification facility; r is the discount rate and is set to be triangularly distributed with a lower limit, mode, and upper limit of 1%, 8%, and 15%, respectively, according to the study by You et al. [13].

3. Results and discussion

3.1 Characteristics of feedstock

Table 2 shows the results from the proximate analysis and ultimate analysis of chicken manure and wood waste. As compared to wood waste, chicken manure contained lower C, H and O content but higher N and ash content. Hence, the HHV of chicken manure is lower (approximately half) than that of wood waste as estimated by Eq. (1). Though the HHV of chicken manure is significantly different (lower) from that of wood waste, co-gasification of these two materials may still be feasible, but it has to be conducted with care (e.g. appropriate mixing ratio of these two feedstocks such that the amount of chicken manure is lesser than wood waste) so as to not severely affect the overall gasification performance. Additionally, when compared to other existing studies [47-49], it was found that the composition of chicken manure could vary significantly especially its C content and hence the HHV, which is not uncommon, mainly due to the different origins and management practices of farm [50].

3.2 Gasification performance

Figure 1(b) shows the transient syngas data from the co-gasification of 30% chicken manure + 70% woodchips recorded by the online gas analyser throughout a period of 15 minutes. When steady state was achieved, the individual syngas data points were averaged over the steady state range to estimate the mean syngas composition. The mean gas composition of the main syngas component (CO and H_2) as well as CH_4 and CO_2 is shown in Figure 1(c). It was observed that the syngas produced from the co-gasification of 30%CM+70%WC had a slightly higher CO and H_2 volume percentage, lower CO_2 volume percentage and similar CH_4 percentage, as compared to the gasification of pure woodchips. Syngas from 30%CM+70%WC contained ~20 vol% CO and ~18 vol% H_2, while syngas from 100%WC contained ~15 vol% CO and ~16 vol% H_2. The remaining components in the syngas generally consist of species that are incombustible such as long carbon chained tar, hydrogen sulphide, carbonyl sulphide, ammonia, nitrogen and other trace contaminants [51]. Overall, the lower heating value (LHV) of the syngas produced from 30%CM+70%WC (5.23 MJ/Nm^3) was comparable to that of 100%WC (4.68 MJ/Nm^3).

The slightly higher LHV of syngas from 30%CM+70%WC could be attributed to the different structure and properties of the feedstock. Firstly, chicken manure is smaller in size, softer and more loosely packed, while wood chips are bigger in size, harder and more compacted. When subjected to gasification, it is hence easier for chicken manure to attain a complete conversion reaction to produce syngas as compared to wood chips. Secondly, wood chips has a higher fixed carbon content than chicken manure. In general, biomass with higher fixed carbon content tend to favour biochar formation [52], which in turn indicates that a lower syngas yield or quality could be expected. Therefore, syngas from the co-gasification of chicken manure and wood chips has more volumetric energy density (MJ/Nm^3) than gasification of pure wood chips.

While the co-gasification of chicken manure and wood chips was only conducted at one mixing ratio (30% chicken manure) due to limited amount of feedstock collected, the performance of other mixing ratios (e.g. 10%, 20% chicken manure) could be inferred from our previous study using food waste [11]. When co-gasified with wood chips at increasing ratio of food waste (0%, 20%, 30% and 40% food waste), the quality of syngas produced in terms of its LHV slightly increased, before encountering the bridging issue due to large amount of undersized particles. As both food waste and chicken manure have similar physical texture, i.e. smaller, softer and more loosely packed than woodchips, such that they are easily reacted completely inside the gasifier to produce syngas, the same increasing LHV trend is expected when their percentage is increased in the feedstock mixture. A comparable and similar quality of syngas was obtained for the co-gasification of 30% food waste and 70% wood chips (LHV 5.27 MJ/Nm^3). All these results showed that chicken manure, like wood chips and food waste, has the right chemical and physical properties for gasification in our gasifier.

In this study, by performing a mass balance, pure wood gasification resulted in approximately 79.8% syngas, 13.9% biochar and 6.3% ash, while co-gasification of chicken manure and wood chips produced about 80.8% syngas, 7.2% biochar and 12.0% ash. The mass fraction of syngas was similar for both cases, while the addition of chicken manure for gasification resulted in a higher mass fraction of ash (lower biochar) than pure wood gasification, mainly due to the high ash content of chicken manure as presented in Table 2. Our finding was somewhat similar with the literature that gasification typically results in roughly 85% gaseous products, 10% solid residue and 5% liquid [53]. It is also known that downdraft gasifier produces lesser tar-oils (<1%) and more particulate matter [54]. Therefore, the amount of liquid produced in this study was assumed negligible.

Last but not least, the raw material to syngas conversion efficiency, or the cold gas efficiency (CGE) for both cases was estimated using Eq. (6)

$$CGE = \frac{LHV_{gas} \times \dot{V}_{gas}}{LHV_{biomass} \times \dot{m}_{biomass}} \times 100\% \tag{6}$$

where LHV_{gas} is the LHV of syngas produced (MJ/Nm^3), $\dot{V}_{gas}$ is the volumetric flow rate of syngas (m^3/hr), $LHV_{biomass}$ is the LHV of biomass (MJ/kg) and $\dot{m}_{biomass}$ is the biomass consumption rate (kg/hr). It was estimated that the CGE was approximately 64.9% and 69.2% for the case of 100%WC and 30%CM+70%WC, respectively. This is similar to the CGE reported in our previous study using the same gasifier for the gasification of woody biomass and mixture with sewage sludge [9]. Though fixed bed downdraft gasifier is known to have a lower efficiency than other gasifiers such as the updraft gasifier due to a high amount of heat being carried over by the hot gas [55, 56], it is still preferred for power generation as the quantity of tar produced is very low [57].

3.3 Characteristics of biochar

The characteristics of the solid residue generated from the gasification experiments, i.e. the biochar, are shown in Table 3. It was noted that the pH of both the biochar (pure woodchips gasification biochar (WC BC) and chicken manure-woodchips co-gasification biochar (CM BC)) was approximately 10, i.e. in the alkaline range. This is consistent with other reported results in the literature that biochar is generally near neutral or alkaline in pH [58, 59]. From the SEM images in Figure 2, though high porosity was observed for both types of biochar, BET analysis showed that their external surface area was quite different. CM BC contained a higher external surface area (340 m^2/g) than WC BC (172 m^2/g), which could be attributed to the different properties of feedstock. In brief, wood chips were bigger in size and had higher fixed carbon content than chicken manure. Hence, it was likely that wood chips experienced a lower burn-off rate compared to the smaller size chicken manure which was more easily and quickly reacted. As such, WC BC had a lower porosity and surface area. This was also reflected by a higher C content remaining in WC BC (84%) compared to that of CM BC (71%). Our finding was similar to the study of Lima et al. [60] where the surface area of their wood shavings biochar was also smaller than that of chicken litter biochar. Nevertheless, the highly porous structure and high surface area of the biochar make it a good adsorbent for the removal of water contaminants such as artificial sweeteners [61-63]. Since CM BC was found to contain higher surface area, it was used for subsequent adsorption study.

3.4 Adsorption kinetics of AS by biochar

Figure 3(a) shows the adsorption kinetics of the 3 AS species (ACE, SAC and CYC) by biochar. In contrast to the typical sorption kinetics that display a smooth L-shape curve with sorption capacity gradually increasing with time, it was observed that the AS kinetic adsorption curve increased very quickly within the first 0.5hr and then slowly plateaued off. This could be due to the absence of the intra-particle surface diffusion owing to the large pore size of biochar, hence there was no rate limiting diffusion step [64]. This is in contrast to the behaviour of a microporous sorbent [65, 66]. Equilibrium was reached approximately within the first two hours of adsorption, with an adsorption capacity of about 30, 50 and 50 mg/kg for ACE, SAC and CYC, respectively. This is also equivalent to a removal efficiency of 82.5%, 98.4% and 65.9% for the three AS species respectively.

From the limited number of such studies in the literature, only one most representative study was found where AS was removed by metal-organic frameworks (MOFs) and activated carbon (AC) [67]. When compared to this study, though the SAC adsorption performance of our biochar was not as superior as the AC, it is noteworthy that the AS concentration used in both studies was different, and AC is a much higher quality and hence expensive material as compared to biochar. Our study used a concentration in the ppb range, a level typically detected in the environment such as surface water or water treatment plants [26, 68], for a more realistic and representative evaluation of the current situation. Furthermore, the benefit of using biochar is to offer low cost adsorptive material that is easily affordable. Nevertheless, this biochar can be upgraded to AC through activation processes [62] at additional costs to further maximize its performance.

In addition, to further examine the kinetic adsorption of AS onto the biochar surface, the AS sorption experimental data at various time points was also fitted into several kinetics models in the literature. Out of the more popular kinetics models such as the first order, second order, and Elovich rate model [69], it was found that the Elovich rate model (Eq. (7)), wherein the model assumes that the adsorption sites are heterogeneous and exhibit a variety of activation energy during the adsorption process [70], provided the best fit for all three AS species.

$$q_t = \frac{1}{\beta}\ln \alpha\beta + \frac{1}{\beta}\ln t \qquad (7)$$

where q_t (mg/kg) is the amount adsorbed/ adsorption capacity , t (hr) is the time, α (mg/kg/hr) is the initial adsorption rate, and β (kg/mg) is the desorption constant. The corresponding R^2 fitting value and the relevant parameters are reported in Table 4. It was found that α was the largest for SAC among the three species, indicating its high initial adsorption rate as shown by the steepest gradient in Figure 3(a). On the other hand, the adsorption of CYC gave the smallest α due to its lower adsorption rate as shown by the curve wherein it was still gradually increasing while the adsorption of SAC and ACE had already plateaued off.

3.5 Adsorption isotherms of AS by biochar

As the adsorption isotherm is commonly used to define the characteristic of solid-liquid adsorption process at equilibrium, the adsorption isotherm study was conducted. Figure 3(b) shows the sorption isotherms of ACE, SAC and CYC by biochar, i.e. the sorption capacity at different equilibrium concentrations. Similarly, the experimental data was fitted to two isotherms models such as the Langmuir model (Eq. (8)) and Freundlich model (Eq. (9)), respectively.

$$S = \frac{S_{\max}KC}{1+KC} \qquad (8)$$

$$S = K_f C^n \qquad (9)$$

where S (mg/kg) is the amount adsorbed/ adsorption capacity , C (ppb) is the equilibrium concentration, $S_{\max}$ (mg/kg) is the maximum amount adsorbed, K (1/ppb) is the Langmuir adsorption constant related to the interaction bonding energy, K_f (mg/kg/ppb^n) is the Freundlich equilibrium constant, and n is the Freundlich linearity constant.

For ACE and CYC, the Langmuir model was found to be a better model to represent their respective adsorption trend (R^2=0.997 for ACE and R^2=0.969 for CYC), whereas SAC was better fitted into the Freundlich model (R^2=0.862). The fitted model parameters of each AS species are shown in Table 5. The fitting results showed that the Langmuir model $S_{\max}$ value was estimated to be larger for ACE than CYC, indicating that the maximum adsorbed amount for ACE was higher than CYC at any given concentration, as represented by its steeper gradient in Figure 3(b). On the other hand, K was smaller for ACE than CYC. This inverse trend is due to the negative correlation between the bonding energy governing the K value and the adsorption maximum $S_{\max}$ [71]. Additionally, it was noted that unlike the typical L-shape of a Langmuir isotherm curve, the Langmuir adsorption isotherms of ACE and CYC were almost linear. This was due to the low concentration of AS used (10-100ppb). At low concentrations, Eq. (8) is simplified into a linear expression.

An equilibrium parameter (R_L) can also be used to express the characteristics of the Langmuir isotherm based on Eq. (10) [72].

$$R_L = \frac{1}{1+K_L C_0} \quad (10)$$

where K_L is the Langmuir isotherm constant and C_0 is the initial concentration. R_L indicates the nature of adsorption where $R_L = 0$ means irreversible, $0 < R_L < 1$ means favourable, $R_L = 1$ means linear, and $R_L > 1$ means unfavourable [73]. Based on the initial concentration range of 10-100ppb used in this study, it was found that the R_L values fall within the range of

0.58-0.99. This indicates that from Langmuir isotherm point of view, biochar is favourable for the adsorption of AS (ACE and CYC) at the experimental conditions used.

3.6 Effect of pH and water hardness on adsorption capacity of AS by biochar

Figure 4(a) shows the adsorption capacity of AS by biochar at different suspension pH. The solution pH is a vital parameter in adsorption process as it affects both the adsorbent (e.g. surface charge) and adsorbate (e.g. ionization and speciation) [74, 75]. The pH at point of zero charge (pH_{pzc}) was approximately pH3.5 (Figure 5). From Figure 4(a), the pH range for this experiment was >pH 3.5 (within pH 7-10). In general, beyond pH_{pzc}, biochar surface charge is net negative. From this test, it was found that adsorption capacity decreases with increasing pH. As pH increases with the addition of alkaline (OH^-), the functional groups (typically phenolic —OH and—COO^- groups) of biochars become more deprotonated [76], hence the overall surface charge is even more negative. This weakens the electrostatic attraction between cationic AS molecules and negative biochar surface. Furthermore, the OH^- ions will compete with anionic AS molecules for adsorption sites. These lead to the decrease in adsorption efficiency. On the other hand, as pH decreases with the addition of acid (H^+), the functional groups are more protonated. Biochar net surface charge becomes less negative (more positive), hence the electrostatic attraction is stronger and the adsorption efficiency increases. This observation suggests that electrostatic interaction could be a mechanism governing the adsorption of AS onto biochar, which is consistent with the findings in literature that electrostatic interaction is the dominant mechanism for the adsorption of organic contaminants onto chars [77]. Figure 4(b) shows the effect of water hardness on the adsorption capacity of AS onto biochar. In general, as water hardness increased, the adsorption efficiency of the three AS species decreased. This is somewhat consistent to the finding reported by Couto et al. where the adsorption of caffeine onto activated carbon decreased under the influence of water hardness, mainly due to the competition effect from calcium and magnesium ions [78].

3.7 Effect of pH on AS-biochar suspension zeta potential

From Figure 5, the pH at point of zero charge (pH_{pzc}) was approximately pH3.5 for both deionized water (control) and AS. When pH> 3.5, zeta potential was negative, indicating that the biochar surface charge was net negative. In general, with increasing pH, the zeta potential became more negative, which suggests that the amount of negative charge increased with pH. Furthermore, in the presence of 100ppb AS, the pH-zeta potential curve shifted slightly to the positive direction. This indicates that there could be some specific bonding or interaction between the AS molecules and the biochar surface such that AS can be specifically adsorbed by biochar. When there is any change in the bonds (e.g. adsorbed ions diffuse into the Stern layer of electric double-layers and form bonds with the biochar surface), the biochar net surface charge will be changed, hence the zeta potential will change as well [79]. Based on this observation, it is hypothesized that specific bonding between AS molecules and functional groups of biochar surface could also be a potential mechanism of adsorption in addition to electrostatic interaction.

3.8 Cost-benefit analysis

The calculated NPV distribution is shown in Figure 6 (a). The average and standard deviation of the NPV distribution are -4.6 million US$ and 21.9 million US$, respectively, over a course of 20 years. Statistically, there is a 41.5% chance for the gasification-based disposal system to bring profit to the farm. Figure 6 (b) shows the comparison among the average cost and benefit components. It is shown that the biochar selling income (53.9 million US$) accounts for the most of the income, followed by the electricity selling income (49.3 million

US$) and waste disposal income (6.0 million US$), respectively. The setting of the variable parameters (e.g., biochar price, electricity tariff, and electrical efficiency) is based on the possible values of recent years, while they may vary significantly depending on the market. The biochar price could be even higher than the ones considered in this work upon the increase of market demand [46, 80, 81]. A 100% increase in the biochar price could increase the profitability probability and average NPV of the gasification system to 93.7% and 49.1 million US$, respectively. Recycling of gasification biochar is important towards the economic feasibility of the gasification system. The increase of electricity tariff could effectively improve the economics of the system. A 100% increase in the electricity tariff could make the system to be 94.2% profitable with an average NPV of 44.2 million US$. Increasing the overall electrical efficiency of the system serves to increase the energy income, which could be achieved by increasing (1) the *CGE* of the gasifier and (2) the *EF* of gas engine. For the former, however, caution needs to be taken because a higher *CGE* generally corresponds to a lower biochar yield (or even a deterioration of biochar quality) and thus less biochar income. This means that the increase of the total income due to the increase of electricity income could be lessened. For the latter, the biochar yield and quality are not affected and the total electricity income will increase. For example, if the *EF* of gas engine increases by 50%, the profitability chance and average NPV of the system increase to 71.7% and 14.3 million US$, respectively. The woodchip cost is the biggest cost component (96.6 million US$) followed by the O&M cost (9.03 million US$) and the facility cost (3.4 million US$). The economics of the system could be improved upon the reduction of the woodchip price or using cheaper alternative co-gasification agents. Halving the woodchip price could increase the profitability chance and average NPV to 99.5% and 45.2 million US$, respectively. Finally, the O & M cost and facility cost may decrease with the continuous advancement of the gasification technology. For example, a 50% decrease in the ratio between the monthly O&M cost and the capital cost increases the profitability probability and the average NPV to 49.7% and -0.38 million US$. On the whole, the economics of the system has a potential to be further improved in the future.

4. Conclusions

In this study, co-gasification of wood waste and chicken manure was conducted in a 10kW fixed-bed downdraft gasifier to evaluate the feasibility of chicken manure as a gasification feedstock. At the same time, the potential of chicken manure as a source for a green and sustainable energy production was studied. The co-gasification test was successfully conducted for a feedstock composition of 30% chicken manure and 70% wood waste. It was found that at 30% chicken manure, the quality of syngas produced in terms of LHV was not significantly different (comparable or slightly higher) from that of pure wood waste gasification, which is an indication that chicken manure is suitable for mixing with wood waste as a feedstock for gasification. This suggests that gasification may be a potential technology for the disposal of chicken manure in a green and environmental friendly way while harnessing clean energy in the form of syngas concurrently.

Furthermore, the biochar produced was found to be able to effectively remove artificial sweeteners (Acesulfame, Saccharin and Cyclamate), a newly categorized class of emerging contaminant, from water via adsorption. Both the kinetics and isotherms sorption behaviors were studied. Based on the effect of pH on the zeta potential of AS-biochar suspension and adsorption efficiency, it is postulated that electrostatic and specific interaction are potential mechanisms governing the adsorption. Last but not least, the cost-benefit analysis showed that there was around 41.5% chance for the system to profit the farm and this probability increases to over 90% if either the biochar price or electricity tariff are doubled, or the woodchip price is halved.

Acknowledgements

This research programme is funded by the National Research Foundation (NRF), Prime Minister's Office, Singapore under its Campus for Research Excellence and Technological Enterprise (CREATE) programme with Grant Number R-706-001-101-281, National University of Singapore.

References

[1] Gerber P, Opio C, Steinfeld H. Poultry production and the environment—a review. Animal Production and Health Division, Food and Agriculture Organization of the United Nations, Viale delle Terme di Caracalla. 2007;153.

[2] USDA. National program 206: Manure and byproduct utilization (FY-2005 Annual Report). 2005.

[3] FarmSafetyAssociation. Manure gas dangers. 2002.

[4] StraitsTimes. Appetite for local produce growing. 2015.

[5] NCCS. Making Waste Work for Us. 2014.

[6] Huang Y, Dong H, Shang B, Xin H, Zhu Z. Characterization of animal manure and cornstalk ashes as affected by incineration temperature. Applied Energy. 2011;88:947-52.

[7] Batterman S. Findings on an Assessment of Small-scale Incinerators for Health-care Waste. World health organization, Geneva. 2004;2004:1-65.

[8] Erlich C, Fransson TH. Downdraft gasification of pellets made of wood, palm-oil residues respective bagasse: experimental study. Applied Energy. 2011;88:899-908.

[9] Ong Z, Cheng Y, Maneerung T, Yao Z, Tong YW, Wang CH, et al. Co-gasification of woody biomass and sewage sludge in a fixed-bed downdraft gasifier. AIChE Journal. 2015;61:2508-21.

[10] Thanapal SS, Annamalai K, Sweeten JM, Gordillo G. Fixed bed gasification of dairy biomass with enriched air mixture. Applied energy. 2012;97:525-31.

[11] Yang Z, Koh SK, Ng WC, Lim RC, Tan HT, Tong YW, et al. Potential application of gasification to recycle food waste and rehabilitate acidic soil from secondary forests on degraded land in Southeast Asia. Journal of environmental management. 2016;172:40-8.

[12] Kan X, Yao Z, Zhang J, Tong YW, Yang W, Dai Y, et al. Energy performance of an integrated bio-and-thermal hybrid system for lignocellulosic biomass waste treatment. Bioresource Technology. 2016.

[13] You S, Wang W, Dai Y, Tong YW, Wang C-H. Comparison of the co-gasification of sewage sludge and food wastes and cost-benefit analysis of gasification-and incineration-based waste treatment schemes. Bioresource technology. 2016;218:595-605.

[14] De Klerk A. Fischer-Tropsch Refining: John Wiley & Sons; 2012.

[15] Hansen V, Müller-Stöver D, Ahrenfeldt J, Holm JK, Henriksen UB, Hauggaard-Nielsen H. Gasification biochar as a valuable by-product for carbon sequestration and soil amendment. Biomass and Bioenergy. 2015;72:300-8.

[16] Rong L, Maneerung T, Ng JC, Neoh KG, Bay BH, Tong YW, et al. Co-gasification of sewage sludge and woody biomass in a fixed-bed downdraft gasifier: Toxicity assessment of solid residues. Waste Management. 2015;36:241-55.

[17] Lehmann J, Joseph S. Biochar for environmental management: science, technology and implementation: Routledge; 2015.

[18] Mohan D, Sarswat A, Ok YS, Pittman CU. Organic and inorganic contaminants removal from water with biochar, a renewable, low cost and sustainable adsorbent–a critical review. Bioresource technology. 2014;160:191-202.

[19] Yao D, Hu Q, Wang D, Yang H, Wu C, Wang X, et al. Hydrogen production from biomass gasification using biochar as a catalyst/support. Bioresource technology. 2016;216:159-64.

[20] Parvage MM, Ulén B, Eriksson J, Strock J, Kirchmann H. Phosphorus availability in soils amended with wheat residue char. Biology and fertility of soils. 2013;49:245-50.

[21] Windeatt JH, Ross AB, Williams PT, Forster PM, Nahil MA, Singh S. Characteristics of biochars from crop residues: potential for carbon sequestration and soil amendment. Journal of environmental management. 2014;146:189-97.

[22] Brewer CE, Levine J. Weight or Volume for Handling Biochar and Biomass? the Biochar Journal. 2015.

[23] Schmidt H-P. The use of biochar as building material. the Biochar Journal. 2014.

[24] Ahmad M, Rajapaksha AU, Lim JE, Zhang M, Bolan N, Mohan D, et al. Biochar as a sorbent for contaminant management in soil and water: a review. Chemosphere. 2014;99:19-33.

[25] Lange FT, Scheurer M, Brauch H-J. Artificial sweeteners—a recently recognized class of emerging environmental contaminants: a review. Analytical and Bioanalytical Chemistry. 2012;403:2503-18.

[26] Sang Z, Jiang Y, Tsoi Y-K, Leung KS-Y. Evaluating the environmental impact of artificial sweeteners: a study of their distributions, photodegradation and toxicities. Water research. 2014;52:260-74.

[27] Wiklund A-KE, Breitholtz M, Bengtsson B-E, Adolfsson-Erici M. Sucralose–An ecotoxicological challenger? Chemosphere. 2012;86:50-5.

[28] Lubick N. Artificial sweetener persists in the environment. ACS Publications; 2008.

[29] Buerge IJ, Buser H-R, Kahle M, Muller MD, Poiger T. Ubiquitous occurrence of the artificial sweetener acesulfame in the aquatic environment: an ideal chemical marker of domestic wastewater in groundwater. Environmental Science & Technology. 2009;43:4381-5.

[30] Mawhinney DB, Young RB, Vanderford BJ, Borch T, Snyder SA. Artificial sweetener sucralose in US drinking water systems. Environmental science & technology. 2011;45:8716-22.

[31] Channiwala S, Parikh P. A unified correlation for estimating HHV of solid, liquid and gaseous fuels. Fuel. 2002;81:1051-63.

[32] Subedi B, Kannan K. Fate of artificial sweeteners in wastewater treatment plants in New York State, USA. Environmental science & technology. 2014;48:13668-74.

[33] Ling R, Yu L, Pham TPT, Shao J, Chen JP, Reinhard M. The tolerance of a thin-film composite polyamide reverse osmosis membrane to hydrogen peroxide exposure. Journal of Membrane Science. 2017;524:529-36.

[34] PUB. Singapore Drinking Water Quality (Jan 2015 - Dec 2015). 2015.

[35] McConnell HM, Morgan KJ, Sine A, Leung YMB, Ward JM, Chilvers BL, et al. Using sea water for cleaning oil from seabird feathers. Methods in Ecology and Evolution. 2015;6:1235-8.

[36] Moghadam RA, Yusup S, Uemura Y, Chin BLF, Lam HL, Al Shoaibi A. Syngas production from palm kernel shell and polyethylene waste blend in fluidized bed catalytic steam co-gasification process. Energy. 2014;75:40-4.

[37] Holmgren KM, Berntsson TS, Andersson E, Rydberg T. Perspectives on investment cost estimates for gasification-based biofuel production systems. Chemical Engineering Transactions. 2015;45:427-32.

[38] Shie J-L, Chang C-Y, Chen C-S, Shaw D-G, Chen Y-H, Kuan W-H, et al. Energy life cycle assessment of rice straw bio-energy derived from potential gasification technologies. Bioresource technology. 2011;102:6735-41.

[39] Suramaythangkoor T, Gheewala SH. Potential alternatives of heat and power technology application using rice straw in Thailand. Applied Energy. 2010;87:128-33.

[40] Palit D, Malhotra R, Kumar A. Sustainable model for financial viability of decentralized biomass gasifier based power projects. Energy Policy. 2011;39:4893-901.

[41] Manzone M. Quality, productivity, energy and costs of woodchip produced by Cedrus deodara plantations: A case study in Italy. Biomass and Bioenergy. 2016;92:81-7.

[42] Kosov V, Lavrenov V, Zaichenko V. Simulation of a process for the two-stage thermal conversion of biomass into the synthesis gas. Journal of Physics: Conference Series: IOP Publishing; 2015. p. 012031.

[43] Yun KT, Cho H, Luck R, Mago PJ. Modeling of reciprocating internal combustion engines for power generation and heat recovery. Applied energy. 2013;102:327-35.

[44] SP. Historical electricity tariff. 2016.

[45] NEA. Refuse disposal facility. 2016.

[46] Ahmed MB, Zhou JL, Ngo HH, Guo W. Insight into biochar properties and its cost analysis. Biomass and Bioenergy. 2016;84:76-86.

[47] Burra K, Hussein M, Amano R, Gupta A. Syngas evolutionary behavior during chicken manure pyrolysis and air gasification. Applied Energy. 2016;181:408-15.

[48] Giuntoli J, De Jong W, Arvelakis S, Spliethoff H, Verkooijen A. Quantitative and kinetic TG-FTIR study of biomass residue pyrolysis: Dry distiller's grains with solubles (DDGS) and chicken manure. Journal of analytical and applied pyrolysis. 2009;85:301-12.

[49] Schnitzer MI, Monreal CM, Facey GA, Fransham PB. The conversion of chicken manure to biooil by fast pyrolysis I. Analyses of chicken manure, biooils and char by 13C

and 1H NMR and FTIR spectrophotometry. Journal of Environmental Science and Health Part B. 2007;42:71-7.

[50] Font-Palma C. Characterisation, kinetics and modelling of gasification of poultry manure and litter: An overview. Energy Conversion and Management. 2012;53:92-8.

[51] Bell DA, Towler BF, Fan M. Coal gasification and its applications: William Andrew; 2010.

[52] Wang L. Sustainable bioenergy production: CRC Press; 2014.

[53] Tripathi M, Sahu J, Ganesan P. Effect of process parameters on production of biochar from biomass waste through pyrolysis: A review. Renewable and Sustainable Energy Reviews. 2016;55:467-81.

[54] Chopra S, Jain A. A review of fixed bed gasification systems for biomass. 2007.

[55] Clark SJ. Thermal biomass gasification. Agricultural Engineering. 1981;62:14-5.

[56] Reed T, Das A. Handbook of biomass downdraft gasifier engine systems: Biomass Energy Foundation; 1988.

[57] Mamphweli NS, Meyer EL. Evaluation of the conversion efficiency of the 180Nm3/h Johansson Biomass Gasifier. International Journal of Energy and Environment. 2010;1:113-20.

[58] Singh B, Singh BP, Cowie AL. Characterisation and evaluation of biochars for their application as a soil amendment. Soil Research. 2010;48:516-25.

[59] Wiedner K, Rumpel C, Steiner C, Pozzi A, Maas R, Glaser B. Chemical evaluation of chars produced by thermochemical conversion (gasification, pyrolysis and hydrothermal carbonization) of agro-industrial biomass on a commercial scale. Biomass and Bioenergy. 2013;59:264-78.

[60] Lima IM, Ro KS, Reddy G, Boykin DL, Klasson KT. Efficacy of chicken litter and wood biochars and their activated counterparts in heavy metal clean up from wastewater. Agriculture. 2015;5:806-25.

[61] Komkiene J, Baltrenaite E. Biochar as adsorbent for removal of heavy metal ions [Cadmium (II), Copper (II), Lead (II), Zinc (II)] from aqueous phase. International Journal of Environmental Science and Technology. 2016;13:471-82.

[62] Maneerung T, Liew J, Dai Y, Kawi S, Chong C, Wang C-H. Activated carbon derived from carbon residue from biomass gasification and its application for dye adsorption: kinetics, isotherms and thermodynamic studies. Bioresource technology. 2016;200:350-9.

[63] Zhang M, Gao B, Varnoosfaderani S, Hebard A, Yao Y, Inyang M. Preparation and characterization of a novel magnetic biochar for arsenic removal. Bioresource technology. 2013;130:457-62.

[64] Inyang M, Gao B, Ding W, Pullammanappallil P, Zimmerman AR, Cao X. Enhanced lead sorption by biochar derived from anaerobically digested sugarcane bagasse. Separation Science and Technology. 2011;46:1950-6.

[65] Axe L, Trivedi P. Intraparticle surface diffusion of metal contaminants and their attenuation in microporous amorphous Al, Fe, and Mn oxides. Journal of Colloid and Interface Science. 2002;247:259-65.

[66] Weerasooriya R, Tobschall HJ, Seneviratne W, Bandara A. Transition state kinetics of Hg (II) adsorption at gibbsite–water interface. Journal of hazardous materials. 2007;147:971-8.

[67] Seo PW, Khan NA, Hasan Z, Jhung SH. Adsorptive Removal of Artificial Sweeteners from Water Using Metal–Organic Frameworks Functionalized with Urea or Melamine. ACS Applied Materials & Interfaces. 2016;8:29799-807.

[68] Scheurer M, Brauch H-J, Lange FT. Analysis and occurrence of seven artificial sweeteners in German waste water and surface water and in soil aquifer treatment (SAT). Analytical and bioanalytical chemistry. 2009;394:1585-94.

[69] Ghaedi M, Nasab AG, Khodadoust S, Rajabi M, Azizian S. Application of activated carbon as adsorbents for efficient removal of methylene blue: Kinetics and equilibrium study. Journal of Industrial and Engineering Chemistry. 2014;20:2317-24.

[70] Acevedo B, Barriocanal C, Lupul I, Gryglewicz G. Properties and performance of mesoporous activated carbons from scrap tyres, bituminous wastes and coal. Fuel. 2015;151:83-90.

[71] Hussain A, Ghafoor A, Anwar-Ul-Haq M, Nawaz M. Application of the Langmuir and Freundlich equations for P adsorption phenomenon in saline-sodic soils. International Journal of Agriculture and Biology. 2003;5:1560-8530.

[72] Fernandez M, Ledesma B, Román S, Bonelli P, Cukierman A. Development and characterization of activated hydrochars from orange peels as potential adsorbents for emerging organic contaminants. Bioresource technology. 2015;183:221-8.

[73] Rozada F, Otero M, García A, Morán A. Application in fixed-bed systems of adsorbents obtained from sewage sludge and discarded tyres. Dyes and pigments. 2007;72:47-56.

[74] Kołodyńska D, Wnętrzak R, Leahy J, Hayes M, Kwapiński W, Hubicki Z. Kinetic and adsorptive characterization of biochar in metal ions removal. Chemical Engineering Journal. 2012;197:295-305.

[75] Li M, Liu Q, Guo L, Zhang Y, Lou Z, Wang Y, et al. Cu (II) removal from aqueous solution by Spartina alterniflora derived biochar. Bioresource technology. 2013;141:83-8.

[76] Yang G, Wu L, Xian Q, Shen F, Wu J, Zhang Y. Removal of Congo Red and Methylene Blue from Aqueous Solutions by Vermicompost-Derived Biochars. PloS one. 2016;11:e0154562.

[77] Inyang M, Gao B, Zimmerman A, Zhang M, Chen H. Synthesis, characterization, and dye sorption ability of carbon nanotube–biochar nanocomposites. Chemical Engineering Journal. 2014;236:39-46.

[78] Couto OM, Matos I, da Fonseca IM, Arroyo PA, da Silva EA, de Barros MASD. Effect of solution pH and influence of water hardness on caffeine adsorption onto activated carbons. The canadian journal of chemical engineering. 2015;93:68-77.

[79] Xu R-k, Xiao S-c, Yuan J-h, Zhao A-z. Adsorption of methyl violet from aqueous solutions by the biochars derived from crop residues. Bioresource technology. 2011;102:10293-8.

[80] Galinato SP, Yoder JK, Granatstein D. The economic value of biochar in crop production and carbon sequestration. Energy Policy. 2011;39:6344-50.

[81] Yoder J, Galinato S, Granatstein D, Garcia-Pérez M. Economic tradeoff between biochar and bio-oil production via pyrolysis. Biomass and Bioenergy. 2011;35:1851-62.

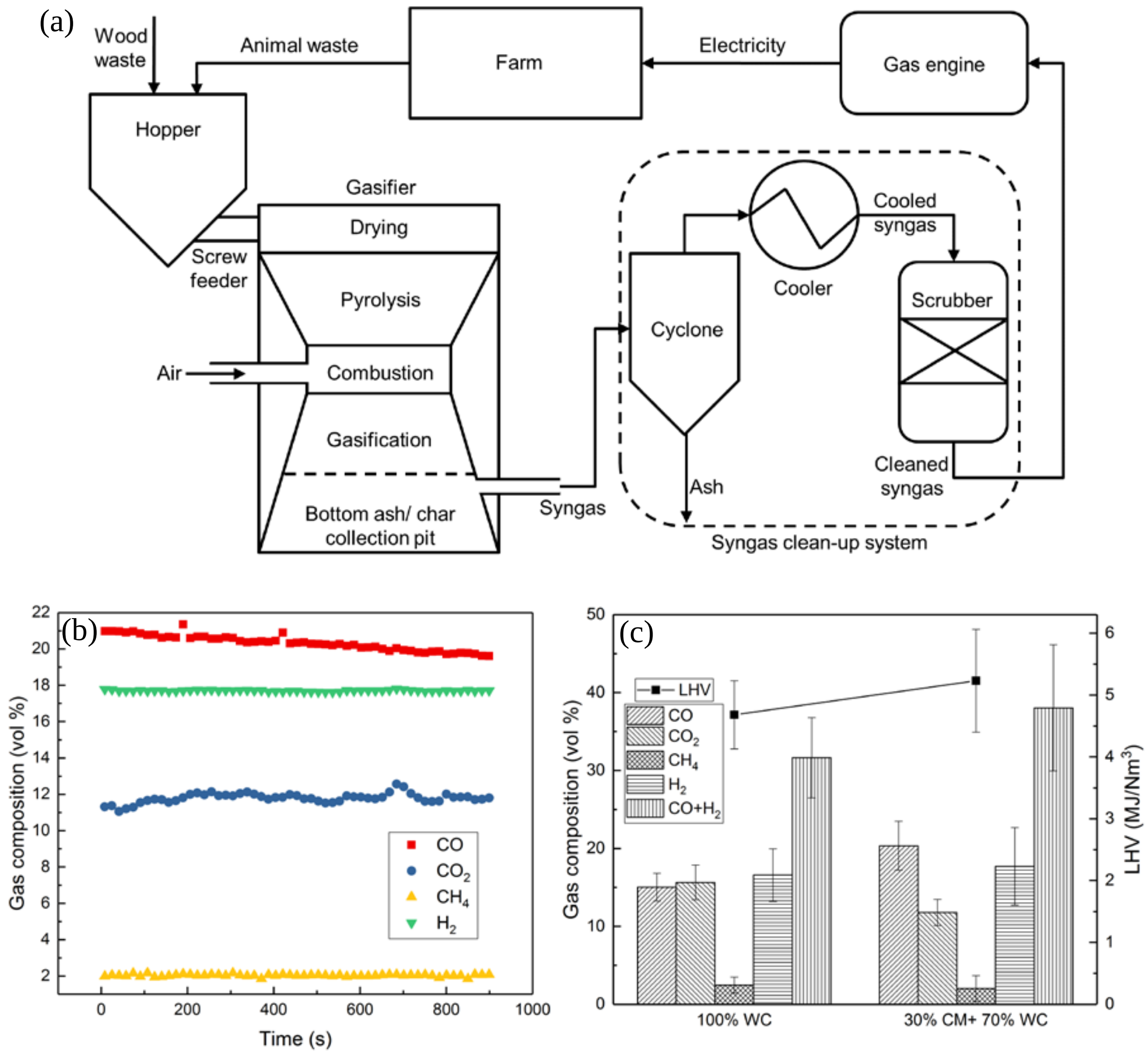

Figure 1. (a) Schematic of fixed-bed downdraft gasifier, and a process flow diagram showing the proposed system for integration of gasifier with other downstream processing units (syngas clean-up and gas engine) for power generation at the farm, (b) Transient syngas data from the co-gasification of chicken manure and woodchips, (c) Syngas composition and its lower heating value (LHV) from the gasification of pure woodchips (100% WC) as compared to the co-gasification of 30% chicken manure and 70% woodchips (30% CM + 70% WC).

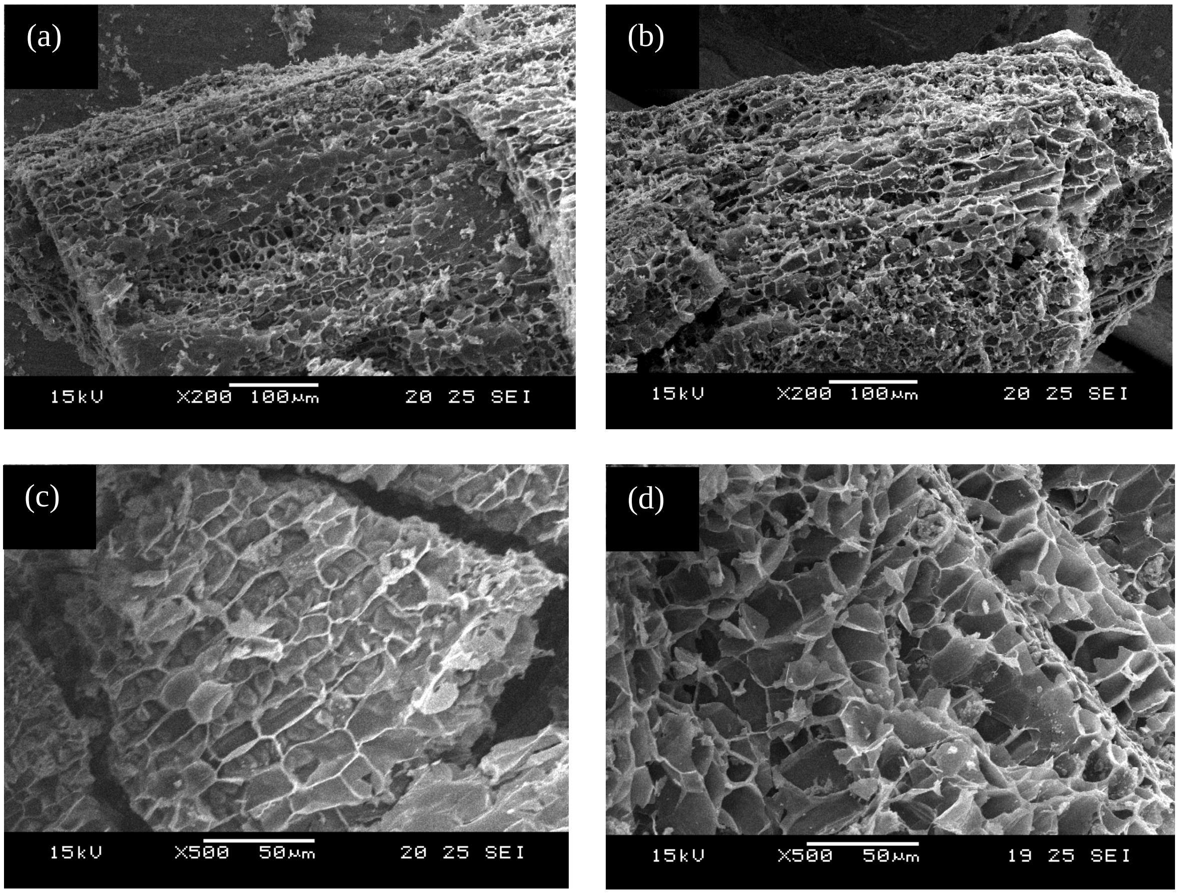

Figure 2. Scanning electron microscopy (SEM) images of biochar from (a, c) pure wood chips gasification, and (b, d) co-gasification of chicken manure and wood chips.

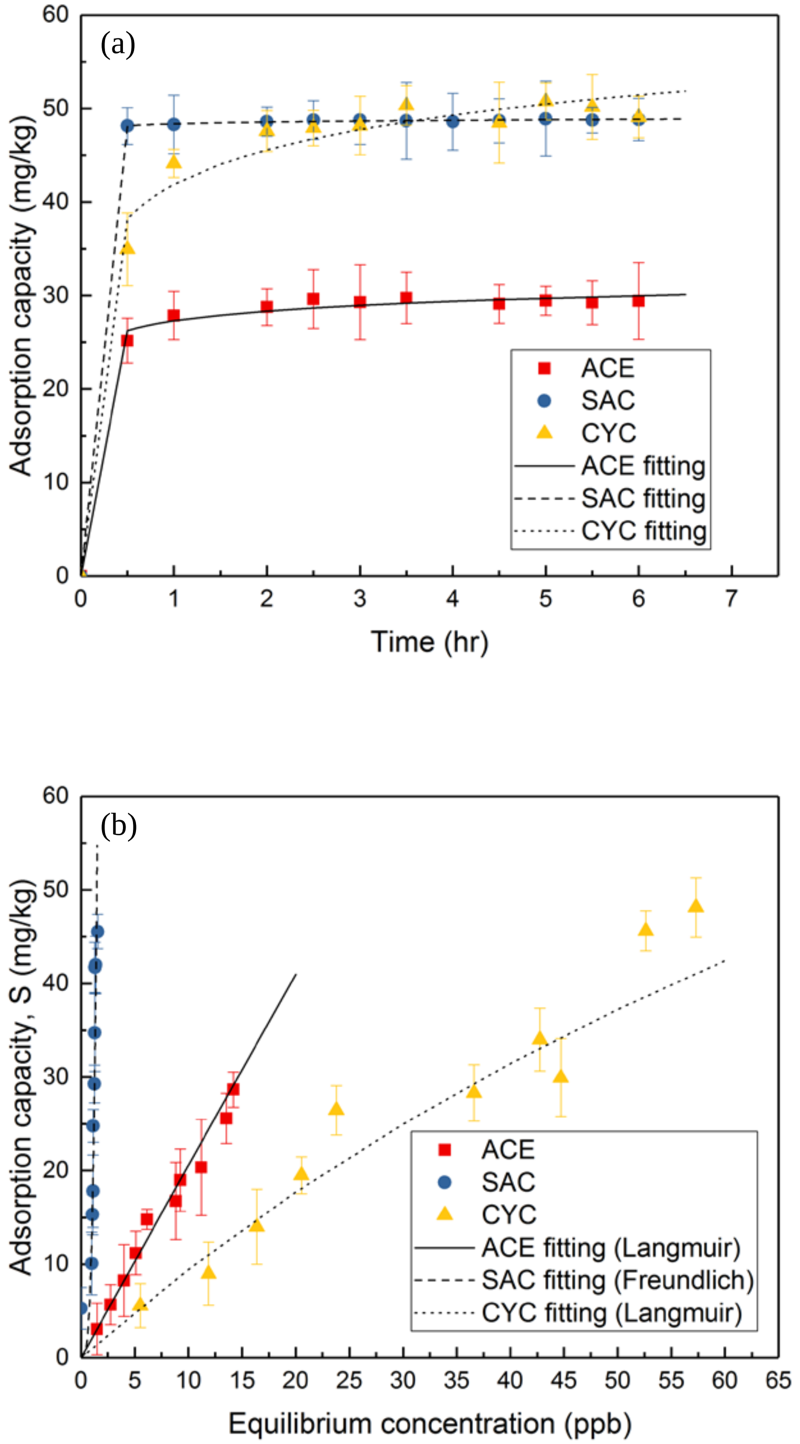

Figure 3. Adsorption of artificial sweeteners by biochar: (a) sorption kinetics, (b) sorption isotherms.

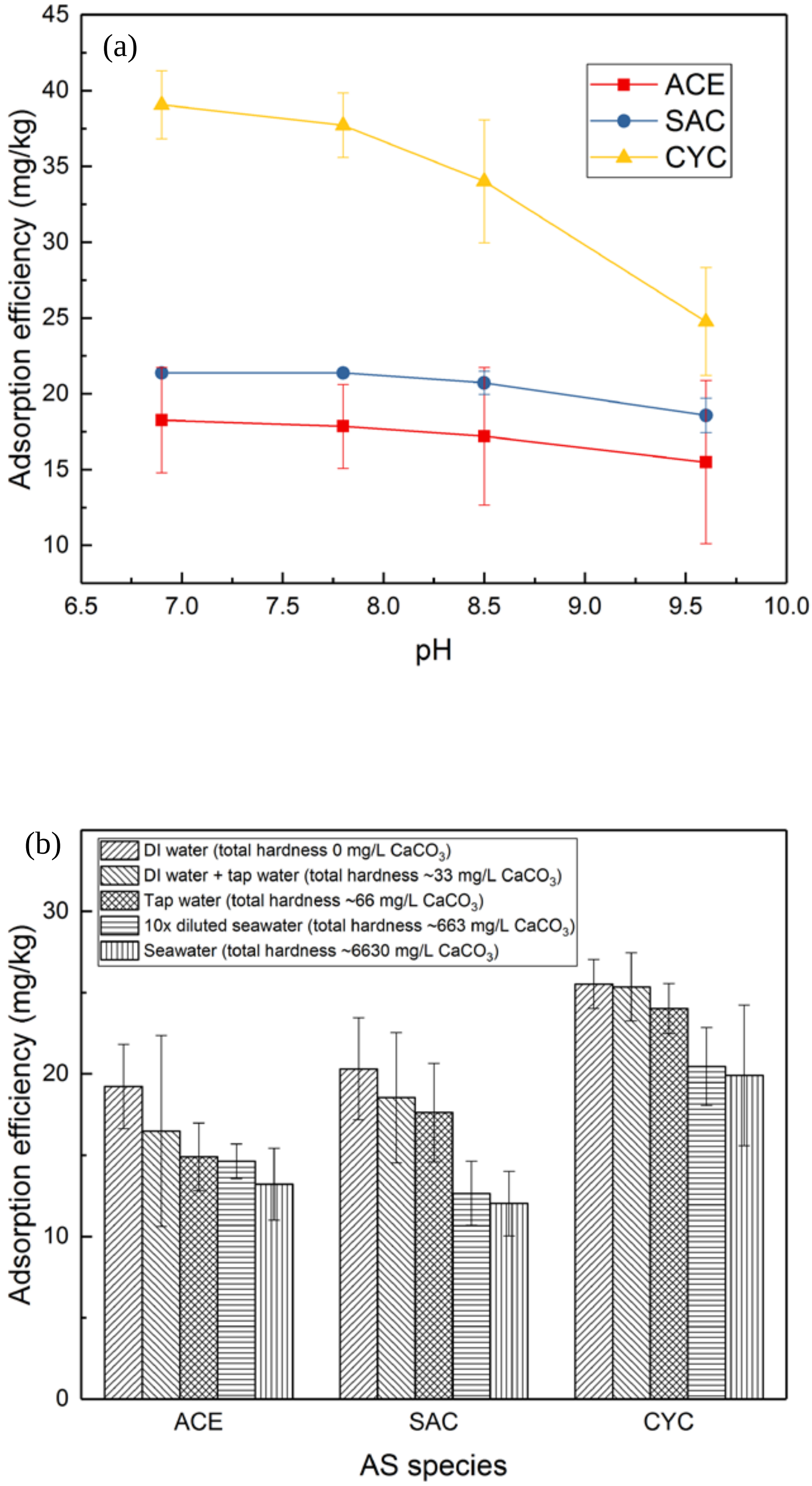

Figure 4. Effect of (a) pH and (b) water hardness on the adsorption efficiency of artificial sweeteners by biochar.

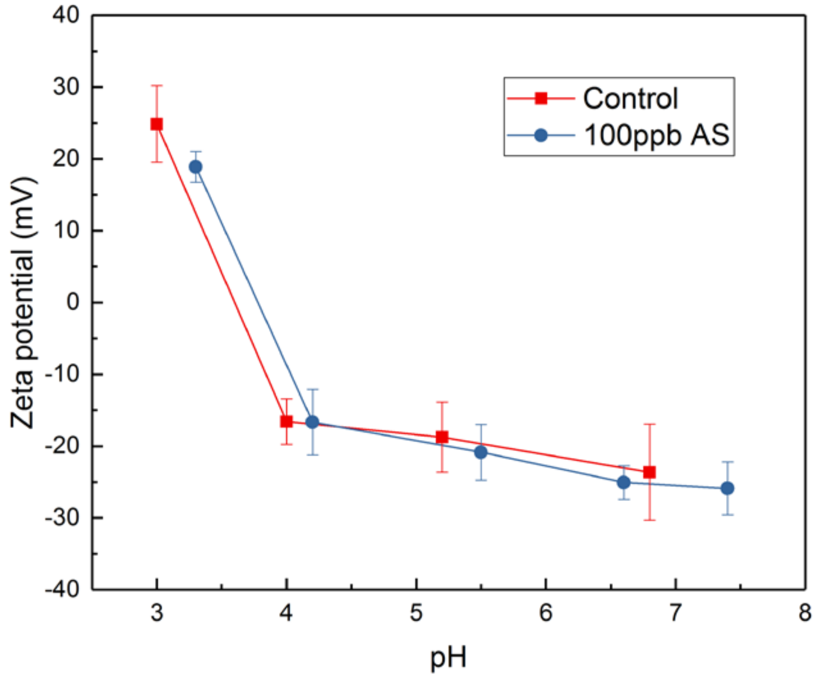

Figure 5. Zeta potential of biochar at different pH.

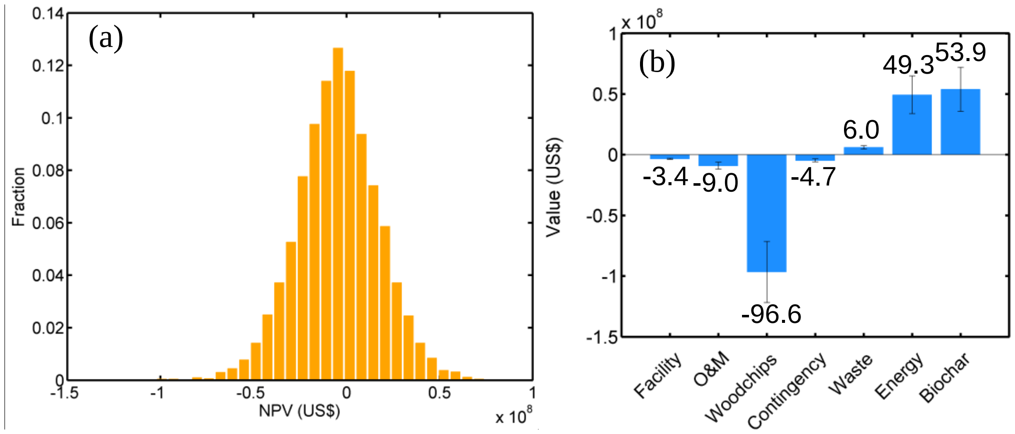

Figure 6. (a) The distribution of NPV. (b) The comparison among average cost and benefit components. The positive values denote benefits while negative values denote costs. The numbers besides the bars in (b) are averages and have the unit of million US$.

Table 1. The lower limit, mode, and upper limit of triangular distributions for cost-benefit analysis using Monte Carlo simulation.

Variable parameters	Lower limit	Mode	Upper limit
Cost of a gasification system in 2007 (US$/kW)	1000	1500	2000
Ratio between monthly O&M cost and capital cost	0.008	0.014	0.02
Cost contingency (US$/kW)	2	4	6
Price of wood chips (US$/ton)	100	150	200
EF (%)	25	35	30
Tariff of electricity (US$/kWh)	0.1	0.2	0.3
Refuse disposal fee (US$/ton)	50	60	70
Price of biochar (US$/ton)	1000	2500	4000
Discount rate (%)	1	8	15

Table 2. Proximate, ultimate analysis and higher heating values of chicken manure and wood waste.

Feedstock	Chicken Manure	Wood Waste
Proximate Analysis (dry basis, wt %)		
Moisture	10.0 (73.6*)	8.3
Volatile	55.2	69.2
Fixed Carbon	9.5	16.2
Ash	25.3	6.3
Ultimate Analysis (dry basis, wt %)		
C	28.2	44.24
H	3.5	6.05
N	8.1	0.86
S	1.1	0.95
O#	33.8	41.60
HHV (MJ/kg)	9.93	18.22

*as received (wet basis) #by difference

HHV= $0.3491 * M_C + 1.1783 * M_H + 0.1005 * M_S - 0.1034 * M_O - 0.0151 * M_N - 0.0211 * M_{ash}$

where M_i : mass fraction of i-th element (i.e. i = C, H, N, S, O and ash) in the waste.

Table 3. Characteristics of biochar

Item		Biochar from chicken manure-wood chips co-gasification (CM BC)	Biochar from pure wood chips gasification (WC BC)
pH		10.12	9.94
Ultimate Analysis (wt%)	C	70.67	84.5
	H	2.06	1.0
	N	0.68	0.5
	S	<0.5	<0.5
Surface Area (m^2/g)		342.26	172.24
Total pore volume (cc/g)		0.224	0.121

Table 4. Kinetics data fitted to Elovich rate model

Species	α (mg/kg/hr)	β (kg/mg)	R^2
ACE	1.37×10^{8}	0.671	0.7624
SAC	1.71×10^{77}	3.704	0.8344
CYC	1.36×10^{4}	0.187	0.8352

Table 5. Isotherms data fitting

Species	Model	S_{max} (mg/kg)	K (1/ppb)	K_f (mg/kg/ppb^n)	n	R^2
ACE	Langmuir	5000	0.0004	-	-	0.9967
	Freundlich	-	-	2.19	0.96	0.9888
SAC	Langmuir	-7.89	-0.62	-	-	0.8103
	Freundlich	-	-	13.19	3.51	0.8623
CYC	Langmuir	140.85	0.0072	-	-	0.9692
	Freundlich	-	-	1.12	0.92	0.9628